RSC Advances

PAPER

View Article Online
View Journal | View Issue

Cite this: *RSC Adv.*, 2017, **7**, 3515

Adjusting the proportions of {0001} facets and high-index facets of ZnO hexagonal prisms and their photocatalytic activity

Yu Liu, Haixia Liu,* Qing Zhang and Tianduo Li

Received 8th October 2016
Accepted 28th November 2016

DOI: 10.1039/c6ra24912d

www.rsc.org/advances

Zinc oxide (ZnO) hexagonal prisms with unique nanostructures are successfully synthesized *via* a simple hydrothermal method with the assistance of polyethylene glycol (PEG). Further studies demonstrated that dissolved PEG played a critical role in adjusting the exposed proportion of {0001} facets and high-index facets. By increasing the amount of PEG, we successfully reduced the exposed proportion of {0001} facets and increased the exposed proportion of high-index facets. The morphology and the properties of ZnO hexagonal prisms were investigated by scanning electron microscopy (SEM), X-ray diffraction (XRD), Brunauer–Emmett–Teller N_2 gas adsorption–desorption isotherms, and photoluminescence (PL) spectra. The photocatalytic activity of the ZnO hexagonal prisms was investigated by photocatalytic degradation of methylene blue (MB) aqueous solution under UV-vis light irradiation. Results showed that the ZnO hexagonal prism samples with a high percentage of exposed high-index facets exhibited superior photocatalytic activity. The idea that adjusting the proportion of different facets to enhance the photocatalytic activity of ZnO samples is a meaningful study.

1. Introduction

There is a growing body of literature that recognises the importance of nanomaterials. Over the past decade, there has been a dramatic increase in the application of photocatalysts.[1] ZnO is one of the most important typical N-type semiconductors with large exciton binding energy (60 meV) and a wide band gap (3.37 eV), which makes it become one of the most popular photocatalysts.[2–4] One of the greatest challenges is the efficiency of photocatalysis. So how to enhance the photocatalytic activity of ZnO nanomaterials is the basis of our study. {0001} facets that are terminated with Zn atoms are the most active facets among the various surfaces of ZnO nanomaterials. So because of the high surface energy of {0001} facets, the exposure of {0001} facets can enhance the efficiency of photocatalysis.[2,5–9] But it is reported that high-index facets also possess high surface energy, so it has huge potential to enhance the efficiency of photocatalysis.[10] In the following of crystal growth habits, the higher energy lattice plane, such as {0001} facets, would grow faster than lower energy lattice plane.[11] Therefore, the result of crystal growth process is that high energy lattice plane is growing fast and disappearing, but low energy lattice plane with slow growth velocity will exposed finally.[12–15] Moreover, previous research has established that surfaces with high energy usually have better properties in photocatalytic reaction.[16] So high-index facets would have good performance on photocatalytic applications.[2]

ZnO is one of the most popular photocatalysts, which can effectively and directly degrade different waste water pollutants through simple photocatalytic oxidation and reduction reactions.[17,18] One major theoretical issue that has dominated the field for many years concerns the photocatalytic activity of as-prepared ZnO nanomaterials. The properties of ZnO nanostructures are more determined by their nanosize, surfaces and quantum effects. So there are various methods have been developed to synthesize ZnO particles with controlled nanostructures. For example, vapor–liquid–solid (VLS) process, chemical vapor deposition (CVD), thermal evaporation, solvothermal methods, hydrothermal methods, ultrasonic irradiation methods. Y. F. Zhu synthesized hierarchical ZnO *via* a two-step chemical route, and the hierarchical ZnO nanostructures could be effectively controlled by changing the composition of solutions.[19] Gastón P. Barreto successfully synthesized hexagonal prismatic particles (100 nm) through the microwave assisted technique.[20] Amin Akbari and his team successfully synthesized ZnO hexagonal plate *via* low temperature hydrothermal method, and the high-resolution TEM images indicate that all the microstructures are single crystals with a [0001] direction growth.[21] Ahmad Umar *et al.* developed a mild hydrothermal method to synthesize ZnO nanoparticles which are based by nanosheets.[22] But all the ZnO nanostructures mentioned above are exposed with {0001} facets or non-active facets. According to previous researches, high-index facets have high surface energy and easily growth rapidly, so it is also

Shandong Provincial Key Laboratory of Fine Chemicals, School of Chemistry and Pharmaceutical Engineering, Qilu University of Technology, Jinan, 250353, P. R. China. E-mail: liuhaixia929@163.com

difficult to synthesis ZnO nanoparticles with exposed high-index facets.[2] Up to now, very little attention has been paid to the role of the proportion in regard to photocatalytic activity. Therefore, how to adjust the proportion of {0001} facets and high-index facets has become the key point of our work.

In this paper, we reported a novel ZnO nanostructure that exposed different proportion of {0001} facets and high-index facets. We successfully adjusted the proportion of {0001} facets and high-index facets *via* changing the amount of PEG in the hydrothermal process. By increasing the amount of PEG, we reduced the percentage of {0001} facets and increased the percentage of high-index facets. The primary aim of this paper is to explore the relationship between the different exposed proportion of facets and photocatalytic activity. The photocatalytic activities of as-synthesized ZnO nanoparticles were investigated by the degradation of methylene blue aqueous under the UV-vis light irradiation. From the view of photocatalytic results, ZnO hexagonal prisms nanoparticles with exposed high percentage of high-index facets showed the greatest photocatalytic activity.

2. Experimental section

2.1 Materials

The starting materials utilized are zinc acetate anhydrous ($C_4H_6O_4Zn$, analysis purity grade, Sinopharm Chemical Reagent Co. Ltd.), 80% ($N_2H_4\cdot H_2O$) and absolute ethanol (Tianjin Fuyu Fine Chemical Co. Ltd.). Polyethylene glycol 2000 (PEG, MW = 2000, Tianjin Damao Chemical Reagent Co. Ltd.) was used as received without further purification. Distilled water was used throughout the experiment.

2.2 Synthesis of ZnO hexagonal prism

In a typical process, 0.03 mol of $C_4H_6O_4Zn$ and 0.1 g PEG was dissolved in 100 mL solution of pure water, then 1.0 mL of $N_2H_4\cdot H_2O$ was dropwise added into the solution at room temperature. The quality of PEG used in the starting solution is changed from 0.5 g to 1.0 g. The mixture was stirred for 30 min after ultrasonic process for 10 min, then transferred into round-bottomed flask (100 mL), and heated at 80 °C for 12 h. These samples were treated by centrifugation and thoroughly rinsed with water and ethanol several times to remove the organic matter, and then dried at 60 °C for 10 h in an oven for subsequent characterization.

2.3 Characterization

XRD patterns were obtained by using a Bruker D8 advanced X-ray powder diffractometer with CuKα radiation (l = 1.5418 Å). The morphologies of ZnO hexagonal prisms were examined by using SEM (Hitachi S-4800 microscope). The Brunauer–Emmett–Teller (BET) specific of the powders was analyzed by using nitrogen adsorption in a nitrogen adsorption apparatus (TriStar II 3020 instrument). All samples were degassed at 100 °C prior to the nitrogen-adsorption measurements. Brunauer Emmett Teller (BET) surface area was determined using adsorption data. Photoluminescence (PL) spectra were measured on a spectrofluorophotometer (F-4600, no. 5J2-0004, Japan) at room temperature.

2.4 Photocatalytic activity

The photocatalytic activities of hexagonal prism ZnO samples were evaluated by degradation of MB aqueous solution under UV-vis light irradiation. 0.1 g of ZnO hexagonal prisms catalysts were added into 100 mL of MB aqueous solution with the initial concentration of 20 mg L^{-1}. Prior to irradiation, the suspensions were stirred magnetically in the dark for 2 h to ensure the establishment of an adsorption–desorption equilibrium. At given irradiation time intervals, 5 mL of the suspensions were collected and then the slurry samples including the ZnO photocatalysts and MB aqueous solution were centrifuged to remove the ZnO catalysts. The Shimadzu UV 2600 UV/Vis spectrophotometer was used to measure the concentration changes of MB solution.

3. Results and discussion

3.1 The property and morphology of ZnO samples

The standard diffraction data for ZnO nanostructures are shown for comparison in Fig. 1. The diffraction peaks were in good agreement with those for ZnO powder obtained from the International Center of Diffraction Data Card (JCPDS no. 36-1451; $P6_3mc$).[23–25] All the diffraction peaks for samples corresponded to those of ZnO with the hexagonal prism structure.[26] By comparing the intensity of peak with different samples, it is obviously to see that the intensity of (002) plane become relative lower with increasing the amount of PEG, which indicates the reducing percentage of {0001} facets. And no other impurity peaks were observed, which indicates the high purity of products.

ZnO nanoparticles synthesized without PEG exhibited the morphology of hexagonal prisms, as shown in Fig. 2a. All the hexagonal prisms with the size of 5.5–6.0 μm possess flat and smooth surfaces. It is shown in Fig. 2c and d that when the amount of PEG was changed from 0 g to 0.5 g, ZnO hexagonal prisms could also obtained. But it can clearly to see that most of

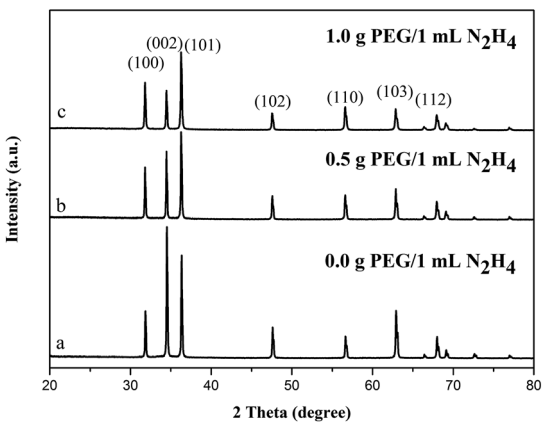

Fig. 1 XRD pattern of different ZnO samples synthesized with different amount of PEG: (a) 0.0 g PEG; (b) 0.5 g PEG; (c) 1.0 g PEG.

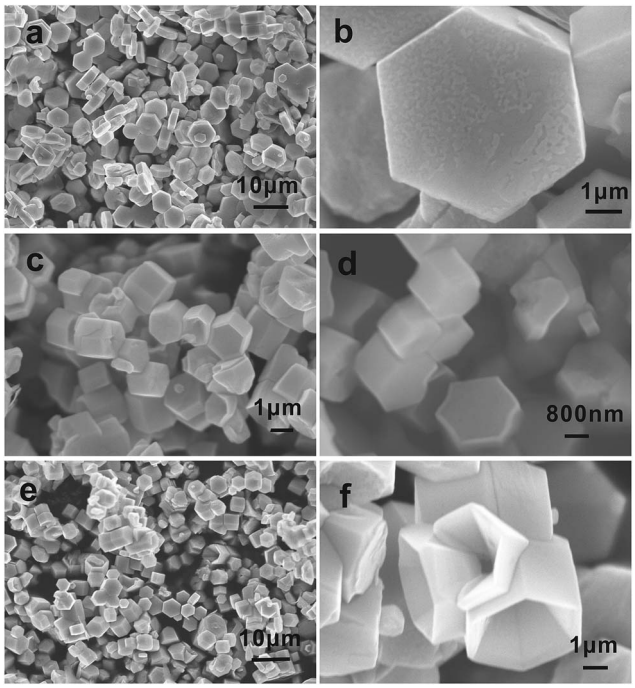

Fig. 2 SEM images of ZnO synthesized with different amount of PEG: (a and b) 0.0 g PEG; (c and d) 0.5 g PEG; (e and f) 1.0 g PEG.

{0001} facets were dented deeply with closer scan of morphology, and arose new high-index facets at the around edge of hexagonal prisms. When with the addition of 1.0 g of PEG, as illustrated in Fig. 2e and f, ZnO nanostructures that exposed {0001} facets and high-index facets were obtained. The most important critical is that the exposed percentage of high-index facets is more than {0001} facets. As a result, we adjusted the proportion of {0001} facets and high-index facets by changing the amount of PEG. It is corresponding with the XRD test results.

3.2 The formation mechanism of ZnO hexagonal prisms

According to the knowledge of the crystallography, the wurtzite ZnO is made up of tetrahedral coordinated zinc and oxygen atoms that are stacked alternately along the *c* axis on structurally.[24] As a consequence, the spontaneous polarization of the {0001} surface and a divergence in a surface energy become the structure feature of ZnO. Moreover, when ZnO crystals exhibit regular hexagonal prism shapes, having $\{1\bar{1}01\}$ planes as the side facets and $\pm\{0001\}$ planes as the top and bottom facets.[27–29] The growth rate is determined by surface energy. Some surfaces with high surface energy would grow fast and disappear, but other surfaces with low surface energy would be exposed finally. There is difference in surfaces energy among surfaces of ZnO samples. So the different growth rate of surfaces results in the diverse morphologies of ZnO samples. In our study, ZnO hexagonal prisms were obtained in the first step. With changing the amount of PEG, the proportion of {0001} facets and high-index facets has changed, as shown in Fig. 3. ZnO hexagonal prisms obtained in the first step, but the dissolved PEG absorbed on {0001} facets and high-index facets in different degrees

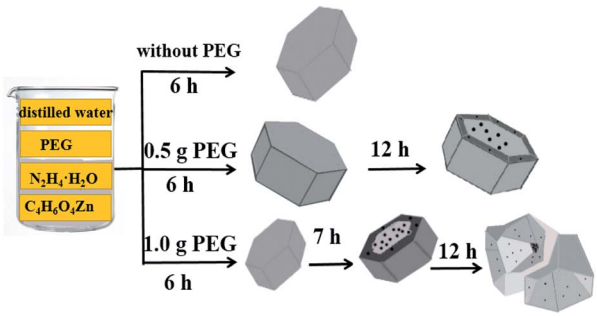

Fig. 3 The growth mechanism of the hexagonal prisms ZnO by the simple schematic.

after the prolonged reaction, which resulting in the different exposed percentage of {0001} facets and high-index facets Therefore, by increasing the amount of PEG, we successfully reduced the percentage of {0001} facets and increased the percentage of high-index facets. It is shown in Fig. 4 that the details about surfaces of ZnO hexagonal prisms. We can clearly to see that the inside bevels are high-index facets and exposed with high percentage in Fig. 4b. So the addition of PEG as variable has become a key factor in the growth of ZnO crystalline. Previous studies have demonstrated that high-index facets are active surfaces because of high surface energy.[2] It has been reported that PEG is a long chain non-ionic surfactant and has hydrophilic –O– and hydrophobic $–CH_2–CH_2–$ radicals on the long chains. When PEG has been well dissolved in water, a good deal of oxygen atoms on PEG chains could easily combine with metal ions to form the flocculated agglomerates.[30]

The reaction equations are summarized as follows:

$$N_2H_4·H_2O = H_3N–NH_2OH \leftrightarrow H_3N–NH_2^+ + OH^- \quad (1)$$

$$Zn^{2+} + 4OH^- = [Zn(OH)_4]^{2-} \quad (2)$$

$$[Zn(OH)_4]^{2-} = Zn(OH)_2 + 2OH^- \quad (3)$$

$$Zn(OH)_2 = ZnO + H_2O \quad (4)$$

$$Zn^{2+} + O^{2-} = ZnO \quad (5)$$

The structure of ZnO could be simply described as a number of alternating planes composed of tetrahedral coordinated O^{2-} and Zn^{2+} ions, stacked along the *c*-axis. The oppositely charged

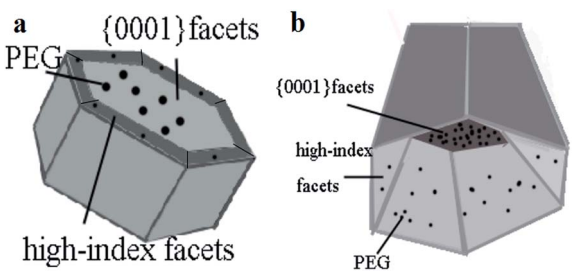

Fig. 4 The enlarged views about the surfaces of ZnO hexagonal prisms: (a) 0.5 g PEG; (b) 1.0 g PEG.

ions produce positively charged {0001} – Zn and negatively charged $\{000\bar{1}\}$ – O polar surfaces, as a result, {0001} facets will enriched with Zn^{2+}.[2] During the reaction, a number of oxygen atoms on the PEG chains could easily react with Zn^{2+} ions. When we added PEG in reaction solution, a large number of oxygen atoms will combine with Zn^{2+} that existed on the {0001} facets. As a result, a lot of PEG adsorbed on {0001} facets and restrain the growth of {0001} facets until the number of O^{2-} were saturated on the {0001} facets. In addition, because the high density of Zn^{2+} and oxygen atoms on the high-index facets, other part of PEG that didn't adsorbed on {0001} facets would adsorbed on the high-index facets instead. In consequence, the present of PEG protect high-index facets to some extent. And ZnO was grown along with *c*-axis as {0001} facets more easily than high-index facets. That's the reason why PEG adsorbed on {0001} facets firstly rather than high-index facets. As shown in Fig. 4, it can clearly to see that PEG adsorbed on {0001} facets and high-index facets in different degree. What's more, the increased amount of PEG more easily adsorbed on high-index facets and restrain the growth of high-index facets. Therefore, we have successfully adjusted the proportion of {0001} facets and high-index facets *via* changing the amount of PEG.

To further investigate the optical performance of ZnO hexagonal prisms, we carried out the PL test to explore the optical properties of ZnO hexagonal prisms. Fig. 5 illustrates the room temperature photofluorescence spectra of ZnO hexagonal prisms under a photo excitation of 325 nm. It can clearly to see that the PL spectra of ZnO hexagonal prisms with the addition of PEG was 1.0 g has a strong ultraviolet (UV) peak at 390 nm, and another PL spectrum corresponding to the ZnO hexagonal prisms with addition of PEG was 0.5 g has a relatively weak UV peak at 379 nm.

By comparison, the position of emission peak arose a red-shift in UV region when we increased the amount of PEG. And the red-shift was caused by quantum size effect of the samples. The absorption peaks view from the (b) line and (a) line at 410–470 nm, 450–480 nm respectively were caused by defects on the surfaces of ZnO nanomaterials. As we all know that the surface states play a crucial role in the PL characteristics of nanomaterials. Due to the adsorption of PEG on the surfaces of ZnO hexagonal prisms, which introduce a lot of defects onto surfaces. That's the reason why we can get absorption peaks at 410–470 nm on the (b) line and 450–480 nm on the (a) line from the PL spectra. These factors may explain the relatively good correlation between PEG and the proportion of {0001} facets and high-index facets.

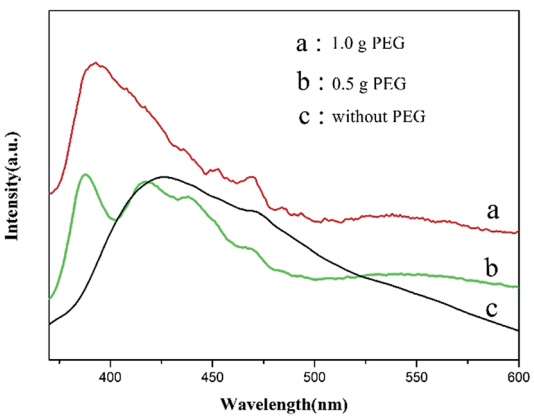

Fig. 5 Room-temperature PL spectra of the ZnO hexagonal prisms with different addition of PEG.

3.3 The photocatalytic activity of ZnO nanostructures

It is known to us all that ZnO has been used as semiconductor photocatalyst for the photocatalytic degradation of organic pollutants in aqueous solution.[12,30] Richa Khokhra *et al.* synthesized ZnO nanosheets by simple soft chemical method and tested their photocatalytic performance. These nanosheets showed high sunlight photocatalytic activity toward the degradation of MB solution, flower-like nanosheets can degrade MB solution up to 79.76% for 120 min of irradiation.[31] Sadia Ameen and his team successfully prepared ZnO nanomaterials by situ polymerization of aniline monomer and applied as a photocatalyst for the degradation of MB solutions. The results showed that the prepared PANI/0.5 wt% ZnO photocatalyst degraded the MB dye by ~76% after 160 min of irradiation.[32] Zhengcui Wu *et al.* developed a general strategy to synthesize Pt or Ag decorated ZnO nanorods arrays through simple chemical solution routes. These hetero-nanostructure arrays show improved photocatalytic activities in the decomposition of RhB dye.[33] And photocatalysis is determined by the excitation of electrons from the valence band to the conduction band of semiconductor materials. When the light of certain wavelength equal or larger than band gap of semiconductor falls on the photocatalyst, which cause the excitation of electrons from valence band to the conduction band and leaving behind the same number of holes (h^+) on the valence band.[31] After the excitation process, electrons and holes transfer from the bulk phase to surface area. A large number of holes with strong oxidizability can oxidate organic pollutants into inorganic substance. This is the reason why ZnO nanomaterials could apply to the treatment of pollutants and protect environment.

The photocatalytic activity of as-prepared ZnO samples, investigated by the photodegradation of MB aqueous solution under the irradiation of UV-vis light, as shown in Fig. 6a. The curves are the concentration of MB aqueous changed under UV-vis light irradiation. The concentration of MB aqueous decreased obviously when ZnO photocatalysts were added to the MB solution, which proved the as-prepared ZnO samples exhibited excellent photocatalytic activity. Fig. 6b shows pseudo-first-rate order kinetics, $\ln(C_0/C) = kt$, for the photocatalytic degradation kinetic reaction. From the formula of pseudo-first-rate, k is a pseudo-first-rate kinetic constant and t is the irradiation time. The calculated degradation rate value for ZnO with the addition of 1.0 g, 0.5 g and 0.0 g PEG were 0.093 min^{-1}, 0.041 min^{-1} and 0.029 min^{-1}, respectively. These results revealed that the ZnO hexagonal prisms that with the addition of 1.0 g PEG exhibited excellent photocatalytic activity.

Thus, compared with the three lines that contained different ZnO catalysts in the text, it is not difficult to find that the photocatalytic activities of ZnO samples were becoming better

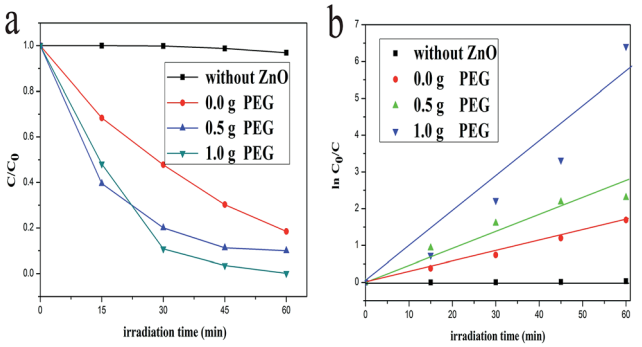

Fig. 6 Photodegradation of MB aqueous solution (a) and kinetics (b) of different ZnO samples as photocatalysts under UV-vis light irradiation.

with the increasing amount of PEG. The existence of PEG enlarged the exposed percentage of high-index facets and reduced the exposed percentage of {0001} facets. On the other hand, the surface areas also increased with the addition of PEG, so we carried out Brunauer–Emmett–Teller N_2 gas adsorption–desorption isotherms test, the BET surface areas of ZnO samples with 0.5 g and 1.0 g PEG were 49.9755 $m^2\ g^{-1}$ and 56.2163 $m^2\ g^{-1}$. The surface areas increased by 12.5%, but the efficiency of the two kinds of ZnO samples was very far apart from each other. The degradation rate of ZnO samples increased by 126%. We found that little increase in surface areas couldn't lead to a huge increase in photocatalytic activity. And the dissolved PEG adsorbed on the high-index facets and introduce a lot of defects, which served as active site for photocatalysis.[13] Therefore, we think that the enhancement in photocatalytic activity not only duo to the increased surface areas, but also mostly attribute to the increase in the proportion of high-index facets. So the as-prepared ZnO samples with 1.0 g PEG showed better photocatalytic activity. After 60 min of UV-vis light irradiation, the degradation percentage of MB aqueous solution by ZnO photocatalyst was up to 95%. Therefore, our ZnO hexagonal prisms with exposed more high-index facets have the greatest photocatalytic activity under UV-vis light irradiation.

4. Conclusions

In summary, this project was undertaken to adjust the proportion of {0001} facets and high-index facets for further evaluate the photocatalytic activity. The most obvious finding to emerge from this study is that the different proportion of {0001} facets and high-index facets could be well controlled *via* changing the amount of PEG. And the as-prepared ZnO hexagonal prisms with exposed high-index facets were successfully synthesized *via* simple hydrothermal method. We can get the conclusion from the results of all the experiments that the interaction of dissolved PEG and zinc species were found to play a great role in adjusting the different proportion of {0001} facets and high-index facets. The more PEG added into the reaction system, the more ZnO hexagonal prisms nanostructure that exposed high-index facets can we obtained. On the promise of increasing surface areas, we also found that ZnO hexagonal prisms samples with exposed high percentage of high-index facets exhibited superior photocatalytic activity. So adjusting the proportion of {0001} facets and high-index facets for the exposed high percentage of high-index facets is beneficial to enhance the efficiency of photocatalysis. The result of this research reveals how to adjust the proportion of {0001} facets and high-index facets of ZnO nanostructures and expand its research scope in the future is a significant work.

Acknowledgements

We acknowledge the financial supports of the National Natural Science Foundation (No. 51402157) and project supported by the outstanding scientific research innovation team plan for university of Shandong Province, China.

Notes and references

1 Z. Y. Jiang, Q. Kuang and Z. X. Xie, *Adv. Funct. Mater.*, 2010, **20**, 3634–3645.
2 H. Y. Tang, Y. Ding, P. Jiang, H. Q. Zhou, C. F. Guo, L. F. Sun, A. F. Yu and Z. L. Wang, *CrystEngComm*, 2011, **13**, 5052–5054.
3 L. L. Wang, J. Ge, A. L. Wang, M. S. Deng, X. J. Wang, S. Bai, R. Li and J. Jiang, *Angew. Chem., Int. Ed.*, 2014, **53**, 1–6.
4 H. S. Jang, B. Son, H. Song, G. Y. Jung and H. C. Ko, *J. Mater. Sci.*, 2014, **49**, 8000–8009.
5 J. X. Sun, Y. P. Yuan, L. G. Qin, X. Jiang, A. J. Xie, Y. H. Shen and J. F. Zhu, *Dalton Trans.*, 2012, **41**, 6756–6763.
6 Y. Z. Chen, D. Q. Zeng, K. Zhang, A. L. Lu and L. S. Wang, *Nanoscale*, 2014, **6**, 874–881.
7 S. S. Ma, J. J. Xue, Y. M. Zhou and Z. W. Zhang, *J. Mater. Chem. A*, 2014, **2**, 7272–7280.
8 T. J. Liu, Q. Wang and P. Jiang, *R. SC. Adv.*, 2013, **3**, 12662–12670.
9 Y. Liu, L. Yu, Y. Hu, C. F. Guo, F. M. Zhang and X. W. Lou, *Nanoscale*, 2012, **4**, 183–187.
10 J. Zhang, R. Ahmed, H. X. Wang, H. W. Liu, R. Z. Liu and P. Wang, *J. Phys. Chem. C*, 2013, **117**, 13836–13844.
11 M. H. Rashid, M. Raula, R. R. Bhattacharjee and T. K. Mandal, *J. Colloid Interface Sci.*, 2009, **339**, 249–258.
12 M. L. Kahn, M. Monge, V. Colliere, F. Senocq, A. Maisonnat and B. Chaudret, *Adv. Funct. Mater.*, 2005, **15**, 458–468.
13 X. J. Wang, Q. L. Zhang, Q. Wan, G. Z. Dai, C. J. Zhou and B. S. Zou, *J. Phys. Chem. C*, 2011, **115**, 2769–2775.
14 G. K. Zhang, X. Shen and Y. Q. Yang, *J. Phys. Chem. C*, 2011, **115**, 7145–7152.
15 K. He, G. L. Zhao and G. R. Han, *CrystEngComm*, 2014, **16**, 3853–3856.
16 Y. Hong, C. G. Tian, B. J. Jiang, A. P. Wu, Q. Zhang, G. H. Tian and H. G. Fu, *J. Mater. Chem. A*, 2013, **1**, 5700–5708.
17 M. Agrawal, S. Gupta, A. Pich, N. E. Zafeiropoulos and M. Stamm, *Chem. Mater.*, 2009, **21**, 5343–5348.
18 P. X. Gao and Z. L. Wang, *J. Am. Chem. Soc.*, 2003, **125**, 11299–11305.
19 Y. F. Zhu, G. H. Zhou, H. Y. Ding, A. H. Liu, Y. B. Lin and N. L. Li, *Phys. E*, 2010, **42**, 2460–2465.

20 G. P. Barreto, G. Morales and M. Luisa López Quintanilla, *J. Mater.*, 2013, 478681.
21 A. Akbari, A. Anaraki Firooz, J. Beheshtian and A. A. Khodadadi, *Appl. Surf. Sci.*, 2014, **315**, 8–15.
22 A. Umar, M. S. Chauhan, S. Chauhan, R. Kumar and S. W. Hwang, *J. Colloid. Interf. Sci.*, 2011, **363**, 521–528.
23 M. Pudukudy, A. Hetieqa and Z. Yaakob, *Appl. Surf. Sci.*, 2014, **319**, 221–229.
24 E. Heredia, C. Bojorge, J. Casanova, H. Canepa, A. Craievich and G. Kellermann, *Appl. Surf. Sci.*, 2014, **317**, 19–25.
25 J. Hu, Y. J. Sun, W. D. Zhang, F. Q. Gao, P. W. Li, D. Jiang and Y. Chen, *Appl. Surf. Sci.*, 2014, **317**, 545–551.
26 Y. N. Xia, P. D. Yang, Y. G. Sun, Y. Y. Wu, B. Mayers, B. Gates, Y. Yin, F. Kim and H. Yan, *Adv. Mater.*, 2003, **15**, 353–389.
27 L. P. Xu, Y. L. Hu, C. Pelligra, C. H. Chen, L. Jin, H. Huang, S. Sithambaram, M. Aindow, R. Joesten and S. L. Suib, *Chem. Mater.*, 2009, **21**, 2875–2885.
28 S. Polarz, *Adv. Funct. Mater.*, 2011, **21**, 3214–3230.
29 S. F. Varol, D. Sahin, M. Kompitsas and G. Cankaya, *RSC Adv.*, 2014, **4**, 13593–13600.
30 Y. J. Feng, M. Zhang, M. Guo and X. D. Wang, *Cryst. Growth Des.*, 2010, **10**, 1500–1507.
31 R. Khokhra, R. Kumar Singh and R. Kumar, *J. Mater. Sci.*, 2015, **50**, 819–832.
32 S. Ameen, M. S. Akhtar, Y. S. Kim, O.-B. Yang and H.-S. Shin, *Colloid Polym. Sci.*, 2011, **289**, 415–421.
33 Z. C. Wu, Y. J. Xue, H. Wang, Y. Q. Wu and H. Yu, *RSC Adv.*, 2014, **4**, 59009–59016.